Varying Appearances of Cholangiocarcinoma: Radiologic-Pathologic Correlation[1]

Yong Eun Chung, MD • Myeong-Jin Kim, MD • Young Nyun Park, MD • Jin-Young Choi, MD • Ju Yeon Pyo, MD • Young Chul Kim, MD • Hyeon Je Cho, MD • Kyung Ah Kim, MD • Sun Young Choi, MD

CME FEATURE

See accompanying test at http://www.rsna.org/education/rg_cme.html

LEARNING OBJECTIVES FOR TEST 2

After reading this article and taking the test, the reader will be able to:

- Discuss the epidemiologic features, risk factors, and morphologic classification of cholangiocarcinoma.
- Describe the typical imaging appearances of cholangiocarcinoma and their correlation with pathologic findings.
- List the findings that can help differentiate cholangiocarcinoma from other benign or malignant diseases.

TEACHING POINTS

See last page

Intrahepatic cholangiocarcinoma is the second most common primary hepatic tumor. Various risk factors have been reported for intrahepatic cholangiocarcinoma, and the radiologic and pathologic findings of this disease entity may differ depending on the underlying risk factors. Intrahepatic cholangiocarcinoma can be classified into three types on the basis of gross morphologic features: mass-forming (the most common), periductal infiltrating, and intraductal growth. At computed tomography (CT), mass-forming intrahepatic cholangiocarcinoma usually appears as a homogeneous low-attenuation mass with irregular peripheral enhancement and can be accompanied by capsular retraction, satellite nodules, and peripheral intrahepatic duct dilatation. Periductal infiltrating cholangiocarcinoma is characterized by growth along the dilated or narrowed bile duct without mass formation. At CT and magnetic resonance imaging, diffuse periductal thickening and increased enhancement can be seen with a dilated or irregularly narrowed intrahepatic duct. Intraductal cholangiocarcinoma may manifest with various imaging patterns, including diffuse and marked ductectasia either with or without a grossly visible papillary mass, an intraductal polypoid mass within localized ductal dilatation, intraductal castlike lesions within a mildly dilated duct, and a focal stricture-like lesion with mild proximal ductal dilatation. Awareness of the underlying risk factors and morphologic characteristics of intrahepatic cholangiocarcinoma is important for accurate diagnosis and for differentiation from other hepatic tumorous and nontumorous lesions.

Abbreviations: BilIN = biliary intraepithelial neoplasia, HCC = hepatocellular carcinoma, H-E = hematoxylin-eosin, PSC = primary sclerosing cholangitis

RadioGraphics 2009; 29:683–700 • **Published online** 10.1148/rg.293085729 • **Content Codes:** GI OI

[1]From the Department of Diagnostic Radiology, Research Institute of Radiological Science (Y.E.C., M.J.K., J.Y.C., Y.C.K., H.J.C., K.A.K., S.Y.C.), Brain Korea 21 Project and Institute of Gastroenterology (M.J.K.), and Department of Pathology (Y.N.P., J.Y.P.), Yonsei University Health System, 250 Seongsanno (134 Sinchon-dong), Seodaemun-gu, Seoul 120-752, Republic of Korea. Received June 10, 2008; revision requested July 28 and received September 17; accepted October 2. All authors have no financial relationships to disclose. **Address correspondence to** M.J.K. (e-mail: *kimnex@yuhs.ac*).

Introduction

Cholangiocarcinomas are malignant tumors arising from the biliary tract (1). Most cholangiocarcinomas are well-, moderately, or poorly differentiated adenocarcinomas with abundant fibrous stroma (2). Intrahepatic cholangiocarcinomas account for 10%–20% of all primary hepatic tumors, with the only curative treatment being complete surgical resection (2–4). Cholangiocarcinomas can be classified into three types on the basis of their gross morphologic features, with each type having its own characteristic imaging findings (5). Cholangiocarcinoma with typical imaging features can easily be diagnosed; however, not all the tumors show typical imaging findings, and the tumors may mimic a variety of tumorous and nontumorous lesions. Understanding the pathologic characteristics of each type of tumor can be helpful in developing a differential diagnosis and in treatment planning. In this article, we discuss and illustrate cholangiocarcinomas in terms of epidemiologic considerations, risk factors, imaging techniques, and morphologic classification with radiologic-pathologic correlation.

Epidemiologic Considerations

Cholangiocarcinoma is the second most common primary malignancy of the liver. The prevalence of cholangiocarcinoma varies markedly from one geographic region to another, with the highest prevalence in Southeast Asia (4,6). Interestingly, recent reports on the epidemiologic features of cholangiocarcinoma in several countries have shown that the prevalence and mortality rates of intrahepatic cholangiocarcinoma are continuously increasing, whereas those of gallbladder and extrahepatic cholangiocarcinoma are remaining constant or decreasing (2). This trend may be attributed in part to the ambiguous classification of hilar cholangiocarcinoma, which has been cross-referenced to both intrahepatic and extrahepatic cholangiocarcinoma but should be classified as extrahepatic cholangiocarcinoma or simply as a separate entity (2,7). A recent epidemiologic study addressed this misclassification issue but showed that the prevalence of intrahepatic cholangiocarcinoma has actually increased, even after the exclusion of the misclassified cases (7).

Teaching Point

Table 1
Risk Factors for Cholangiocarcinoma

Liver flukes (*Opisthorchis viverini, Clonorchis sinensis*)*
Hepatolithiasis (recurrent pyogenic cholangitis)*
Primary sclerosing cholangitis (PSC)†
Viral infection (human immunodeficiency virus, hepatitis B virus, hepatitis C virus, Epstein-Barr virus)
Anomaly and malformation (anomalous pancreaticobiliary junction and choledochal cyst, fibrocystic liver diseases [eg, Caroli disease])
Environmental or occupational toxin (thorotrast, dioxin, polyvinyl chloride)
Biliary tract–enteric drainage procedures
Heavy alcohol consumption

Note.—All risk factors listed share the common feature of chronic biliary inflammation.
*More common in Eastern countries.
†More common in Western countries.

Risk Factors

Teaching Point

There are a number of recognized risk factors for cholangiocarcinoma that all share the common feature of chronic biliary inflammation (Table 1). Among these risk factors, infection with liver flukes (eg, *O viverini* and *C sinensis*) and hepatolithiasis are common causes of cholangiocarcinoma in endemic areas. Dietary or endogenous nitrosamine compounds associated with parasitic infections also play an important role as cofactors in carcinogenesis, probably due to the carcinogenic effect of nitrosamine compounds on the proliferation of epithelial cells of the bile duct (2,8). At imaging, the association of cholangiocarcinoma with clonorchiasis may be characterized by prominent ductal dilatation, not only in the peritumoral area but also in remote areas of the liver. At microscopic examination, a degenerated larva may be seen within the dilated duct with marked periductal fibrosis and inflammatory reaction (Fig 1) (9). Innumerable eggs can also be present in the ductal lumen. Hepatolithiasis is another common risk factor in parts of Asia, especially Japan, Taiwan, China, and Korea (2,4,10,11). Up to 10% of cases of intrahepatic stone disease are complicated by cholangiocarcinoma, and up to 70% of cholangiocarcinomas manifest with intrahepatic stone disease in endemic areas (Fig 2) (2). The mean time lag between the diagnosis of intrahepatic stone dis-

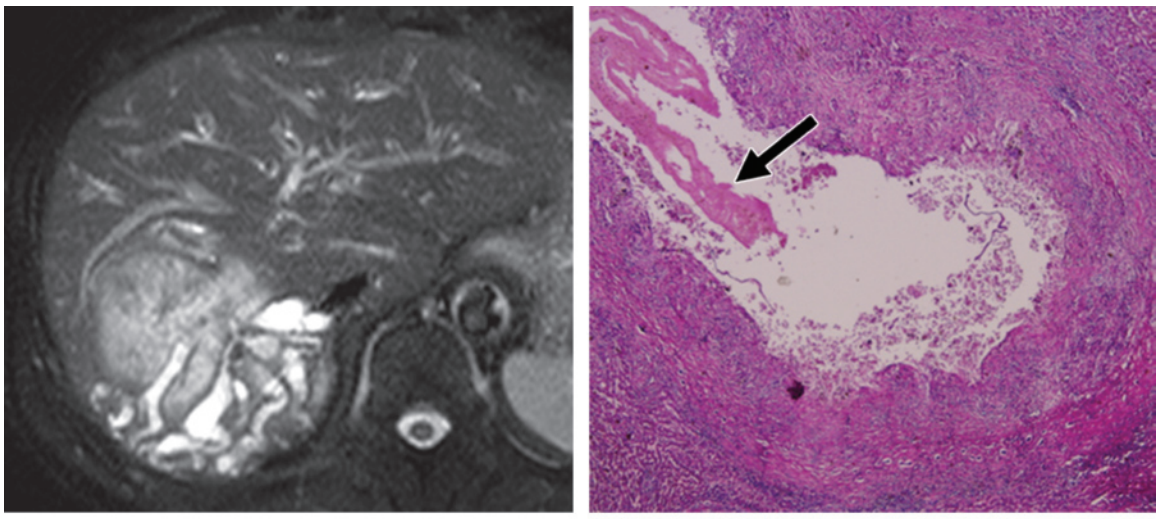

a. b.

Figure 1. Mass-forming cholangiocarcinoma in a patient with clonorchiasis. **(a)** Axial fat-suppressed T2-weighted magnetic resonance (MR) image shows a hyperintense mass, with marked intrahepatic biliary dilatation in the mass and the adjacent liver. **(b)** Photomicrograph (original magnification, ×40; hematoxylin-eosin [H-E] stain) shows a degenerated parasitic larva (arrow) and marked periductal fibrosis.

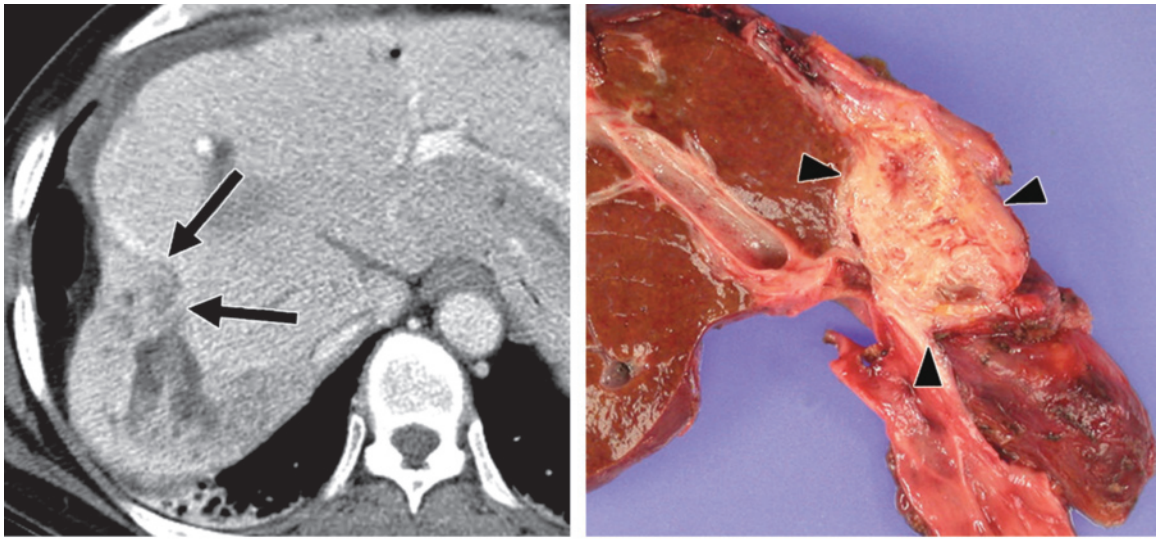

a. b.

Figure 2. Mass-forming cholangiocarcinoma. **(a)** Contrast material–enhanced computed tomographic (CT) scan shows bile duct dilatation with a poorly enhancing lesion in the adjacent liver (arrows). There is significant parenchymal atrophy with capsular retraction peripheral to the more centrally located cholangiocarcinoma. **(b)** Photograph of the gross specimen clearly depicts a large mass (arrowheads) around the sclerotic bile duct.

ease and the development of cholangiocarcinoma is about 8 years, and tumors may develop even after complete stone removal (12). At CT, cholangiocarcinoma associated with hepatolithiasis can be seen as periductal soft-tissue attenuation or ductal wall thickening with dilatation, with or without bile duct stricture. On contrast-enhanced portal venous phase scans, the involved intrahepatic bile duct may show a higher enhancement than the adjacent normal bile duct. Portal vein

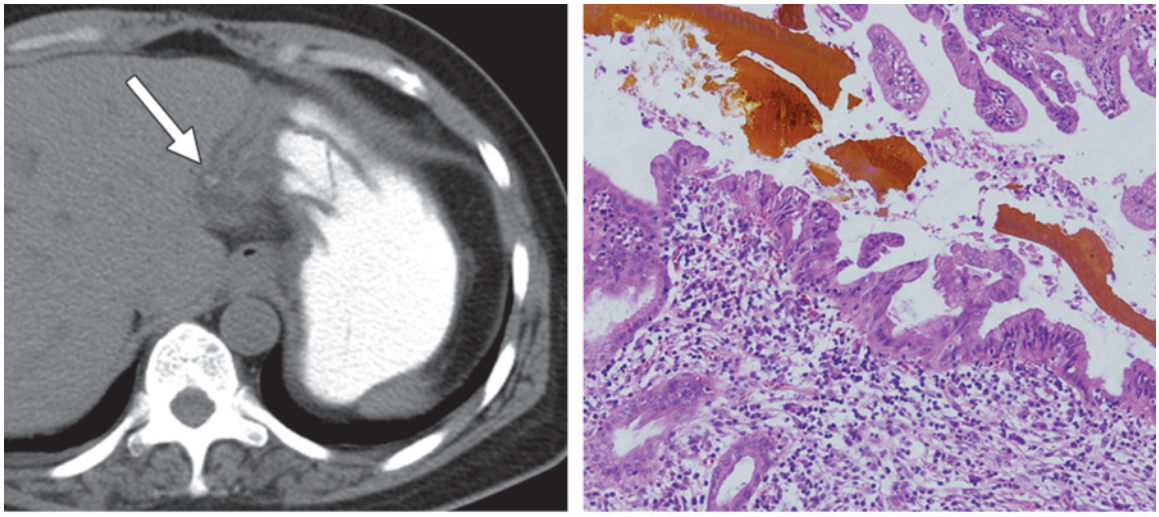

a. b.

Figure 3. BilIN in a patient with intrahepatic stone disease. **(a)** Axial precontrast CT scan shows hepatolithiasis (arrow) in the dilated left intrahepatic duct. **(b)** Photomicrograph (original magnification, ×100; H-E stain) shows dysplastic changes along the bile duct epithelium, a finding known as biliary dysplasia or BilIN.

obliteration, hepatic lobe atrophy, and cholangitic abscess can also occur (13,14). In patients who undergo surgery for intrahepatic stone disease without cholangiocarcinoma, biliary intraepithelial neoplasia (BilIN) is commonly seen in the surgical specimen (Fig 3). BilIN is considered to be a precursor lesion of cholangiocarcinoma and is characteristically a microscopic lesion with a flat or micropapillary dysplastic epithelium known as biliary dysplasia, atypical biliary epithelium, or carcinoma in situ (15).

In Western countries, PSC is one of the most common risk factors for cholangiocarcinoma. Cholangiocarcinoma develops at an earlier age than does sporadic disease (usually within 2 years of the diagnosis of PSC), and the risk of cholangiocarcinoma is not related to the duration or severity of PSC or inflammatory bowel disease (2). At CT, cholangiocarcinoma with underlying PSC has been noted as a hypoattenuating mass or thickened bile duct wall (16). In countries where hepatolithiasis and liver fluke infection are rare, the epidemiologic features of cholangiocarcinoma are not well understood. A recent study from the United States showed that liver cirrhosis, chronic hepatitis C viral infection, and heavy alcohol consumption are risk factors in these countries (17). In addition, a European study showed that a history of alcohol-related liver disease, cirrhosis, various bile duct diseases, chronic inflammatory bowel disease, or diabetes may increase the risk of development of cholangiocarcinoma (18). In our experience, cholangiocarcinomas occurring in association with chronic liver disease are frequently small, possibly because the patients are in a surveillance program. A small cholangiocarcinoma may manifest as a hypervascular tumor, whereas most of the large mass-forming tumors manifest as a predominantly hypovascular mass with a hypervascular rim (19). Cholangiocarcinoma arising from a cirrhotic liver may be surrounded by a fibrotic pseudocapsule, which is an unusual finding in cholangiocarcinoma arising from a noncirrhotic liver. In such cases, capsular retraction is noted along the tumor surface. This capsular retraction may be seen in some hepatocellular carcinomas (HCCs) with cirrhotic stroma but is more suggestive of cholangiocarcinoma (Fig 4).

Cholangiocarcinoma can develop in a congenital choledochal cyst, with a lifetime risk of 10%–15% (3,20). Surgery is the treatment of choice, but excision of the choledochal cyst cannot completely prevent carcinogenesis. Cholangiocarcinoma developed in about 1% of the patients who underwent surgery (21). Combined infected bile stasis and gallstones has been suggested as a cause of malignant change in the remaining bile duct (21).

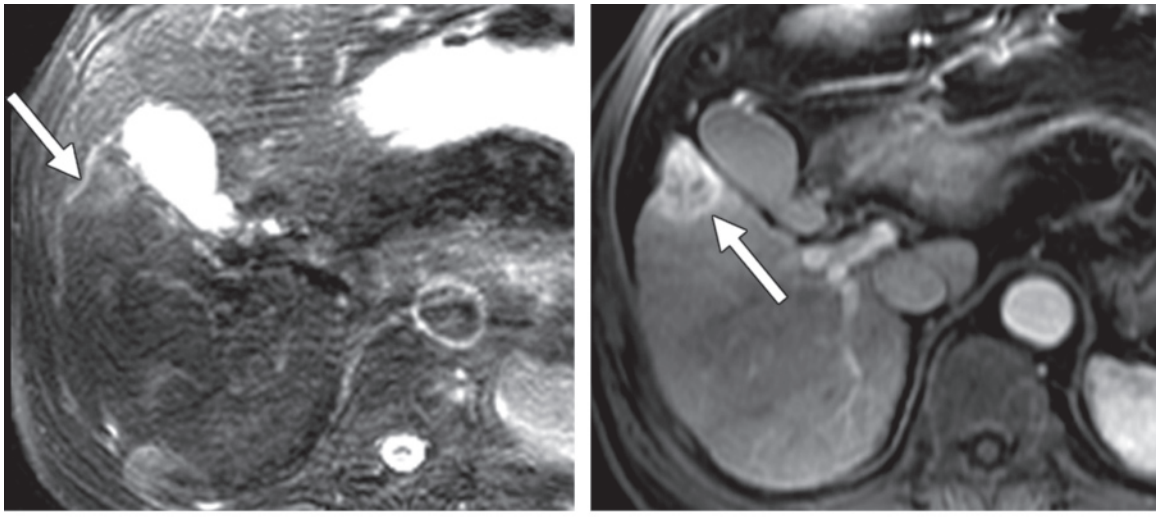

a. b.

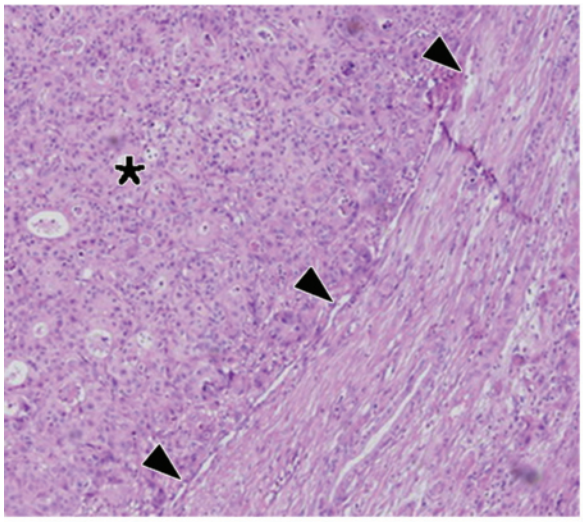

c.

Figure 4. Mass-forming cholangiocarcinoma arising in a cirrhotic liver. **(a)** Axial fat-suppressed T2-weighted MR image shows a slightly hyperintense mass with capsular retraction (arrow) in segment V of the liver. **(b)** Contrast-enhanced arterial phase T1-weighted MR image shows strong enhancement of the tumor (arrow). **(c)** Photomicrograph (original magnification, ×100; H-E stain) shows a fibrotic pseudocapsule (arrowheads) surrounding the tumor (*).

Imaging Techniques

Although multidetector CT is widely used, multiphase scanning is possible without a reduction in spatial resolution or scanning range. At our institution, precontrast and triphasic CT, including late arterial phase, hepatic venous phase, and equilibrium phase scanning, is usually performed in a patient who has not undergone prior CT. Precontrast CT is useful for the detection and differentiation of an intraductal stone. In patients with an intraductal mass at postcontrast scanning, it is often hard to differentiate between an intraductal tumor and an intraductal stone without a precontrast image (22,23). Late arterial phase CT performed 20–30 seconds after contrast medium injection is useful for understanding the arterial anatomy and planning the surgical method (24). Hepatic venous phase CT is performed 25–30 seconds after the completion of late arterial phase scanning. At hepatic venous phase scanning, cholangiocarcinoma shows a higher enhancement than does the adjacent normal liver parenchyma or normal bile duct (25–27). At delayed phase scanning (performed 150–180 seconds after the completion of hepatic venous phase scanning), cholangiocarcinoma commonly shows a higher attenuation than does the surrounding liver, a finding that is related to abundant fibrous stroma. Delayed phase scanning performed 3–30 minutes after contrast medium injection can demonstrate late enhancement of the tumor, a finding that reflects abundant fibrous stroma within the tumor in intrahepatic or hilar cholangiocarcinoma, but it is not widely used for the evaluation of extrahepatic cholangiocarcinoma (28,29). The MR imaging protocol at our institution includes axial and

coronal T2-weighted images, a fat-saturated T1-weighted image, a dynamic contrast-enhanced T1-weighted image obtained with a bolus tracking technique, and MR cholangiopancreatography. The T2-weighted images and the dynamic contrast-enhanced T1-weighted MR image can be helpful for detecting and characterizing the tumor (30). Contrast-enhanced MR imaging is also useful in differentiating between benign and malignant bile duct strictures (31,32). MR cholangiopancreatography is helpful in the evaluation of a periductal infiltrating or intraductal growth type tumor (33,34).

Morphologic Classification: Radiologic-Pathologic Correlation

According to the morphologic classification system proposed by the Liver Cancer Study Group of Japan (5), cholangiocarcinoma is classified into mass-forming, periductal infiltrating, and intraductal growth types (Fig 5). Traditionally, extrahepatic bile duct cancer has been classified as nodular, sclerosing, or papillary (3), corresponding to the mass-forming, periductal infiltrating, and intraductal growth types of intrahepatic cholangiocarcinoma, respectively. Classification based on gross morphologic characteristics is valuable for the interpretation of imaging features and the development of a differential diagnosis. It is also useful for predicting tumor dissemination and prognosis and for planning the surgical approach (35–37).

Mass-forming Type

Mass-forming cholangiocarcinoma is characterized morphologically by a homogeneous mass with an irregular but well-defined margin and is frequently associated with dilatation of the biliary trees in the tumor periphery. Vascular encasement by the tumor is also common, but grossly visible intravascular tumor thrombosis is rare. At ultrasonography (US), mass-forming cholangiocarcinoma manifests as a homogeneous mass with an irregular but well-defined margin. A peripheral hypoechoic rim is seen in about 35% of all tumors and consists of compressed liver parenchyma or proliferating tumor cells (38). Tumors greater than 3 cm in size are usually hyperechoic, but tumors less than 3 cm are hypo- or isoechoic

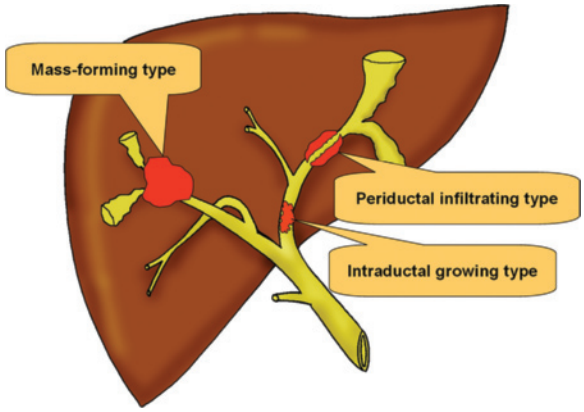

Figure 5. Drawing illustrates the three types of cholangiocarcinoma according to the morphologic classification system proposed by the Liver Cancer Study Group of Japan.

(39). The typical CT features of a mass-forming cholangiocarcinoma include homogeneous attenuation, irregular peripheral enhancement with gradual centripetal enhancement, capsular retraction, the presence of satellite nodules, and vascular encasement without the formation of a grossly visible tumor thrombus (Fig 6a–6c) (40–43). Other common findings include the presence of hepatolithiasis associated with the ductal dilatation and obliteration of the portal vein, leading to atrophy of the involved segment (44). At gross examination, mass-forming cholangiocarcinoma is characterized by a homogeneous sclerotic mass with an irregular lobulated margin, typically in the absence of hemorrhage or central necrosis (Fig 6d) (42). At histologic analysis, the viable tumor cells are usually located at the periphery of the tumor. The central portion of the tumor is composed of a variable degree of fibrosis and shows coagulative necrosis with scanty scattered tumor cells (Fig 6e, 6f) (30). The degree of enhancement of a tumor on the delayed phase image, which is usually obtained 3–15 minutes after contrast medium administration, is closely related to the amount of interstitial space in the fibrous stroma. Valls et al (45) reported that 81.8% of tumors with severe fibrosis showed delayed enhancement, whereas none of the tumors in patients without fibrosis showed delayed hyperenhancement.

Teaching Point

The MR imaging features of mass-forming cholangiocarcinoma are similar to its CT features (30,33,44). The mass shows an irregular margin with high signal intensity at T2-weighted imaging

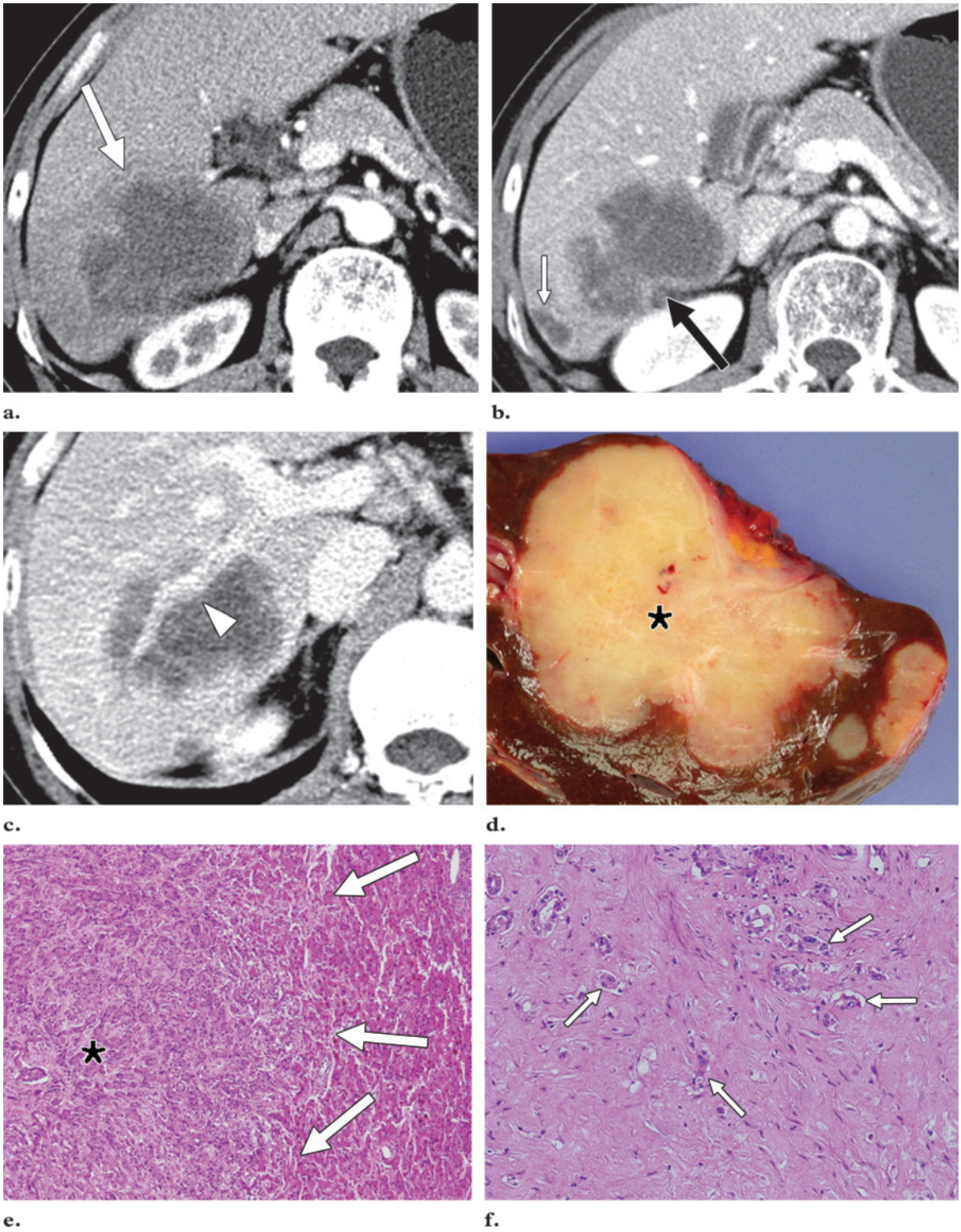

Figure 6. Typical features of mass-forming cholangiocarcinoma at CT, gross examination, and histologic analysis. **(a)** Arterial phase CT scan shows a tumor with ragged rim enhancement at the periphery (arrow). **(b)** Axial portal venous phase CT scan shows gradual centripetal enhancement of the tumor with capsular retraction (black arrow). A satellite nodule is also seen (white arrow). **(c)** Three-minute delayed phase CT scan shows gradual centripetal enhancement with tumor encasement of the posterior branch of the right portal vein (arrowhead). Encasement of a portal or hepatic vein without formation of a grossly visible tumor thrombus is one of the distinguishing features of cholangiocarcinoma as opposed to HCC. **(d)** Photograph of the gross specimen shows a homogeneous sclerotic mass with an irregular infiltrative margin and a central area of whitish scarred tissue (*), findings that correlate well with microscopic findings, namely, tumor cells that are more prominent at the periphery of the mass, with fibrotic stroma being more prominent in the center of the tumor. **(e)** Photomicrograph (original magnification, ×40; H-E stain) of the periphery of the tumor shows the indistinct tumor margin, in which tumor cells (*) are intermingled with normal hepatocytes in the adjacent liver (arrows). **(f)** Photomicrograph (original magnification, ×100; H-E stain) of the inner portion of the tumor shows a larger amount of fibrous tissue with scattered tumor cells (arrows).

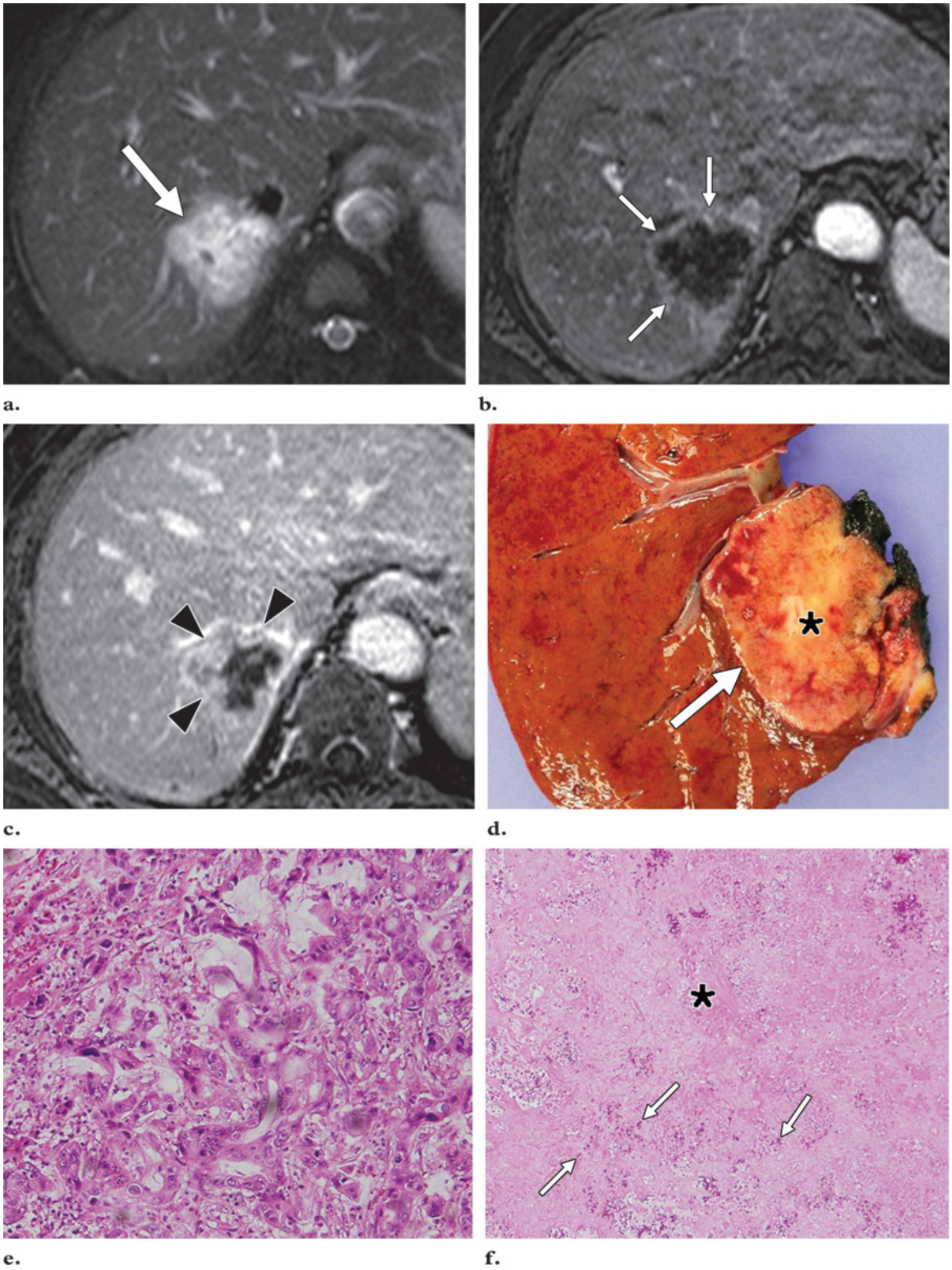

Figure 7. Typical MR imaging features of mass-forming cholangiocarcinoma. **(a)** Axial fat-suppressed T2-weighted MR image shows a high-signal-intensity lobulated mass in the right hepatic lobe (arrow). **(b, c)** Contrast-enhanced arterial phase **(b)** and equilibrium phase **(c)** T1-weighted MR images show irregular, ragged rim enhancement (arrows in **b**) with gradual centripetal enhancement (arrowheads in **c**). **(d)** Photograph of the gross specimen shows a mass with a relatively homogeneous appearance (arrow), although the central area of the tumor is somewhat whitish (*). **(e)** Photomicrograph (original magnification, ×100; H-E stain) of the tumor periphery shows a moderately differentiated adenocarcinoma, a finding that is consistent with the peripheral rim enhancement seen in **b** and **c**. **(f)** Photomicrograph (original magnification, ×40; H-E stain) of the central portion of the tumor shows coagulative necrosis (*) with scanty tumor cells (arrows).

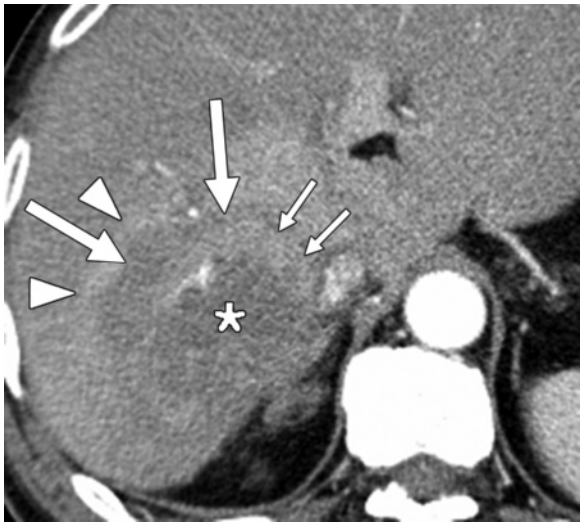

Figure 8. Hepatic tuberculosis. Contrast-enhanced arterial phase CT scan shows four layers of hepatic tuberculosis. Microscopic examination showed the outermost (hyperattenuating) layer (arrowheads) to consist of compressed normal hepatic parenchyma with sinusoidal dilatation, the second (hypoattenuating) layer (large arrows) to consist mainly of fibrosis, the third (hyperattenuating) layer (small arrows) to represent granulomatous inflammation, and the innermost (hypoattenuating) layer (*) to represent caseous necrosis.

and with low signal intensity at T1-weighted imaging. Both the peripheral and the centripetal enhancement may be more prominent at MR imaging than at CT (Fig 7). In certain cases, prominent central enhancement can be seen on the equilibrium phase or delayed phase MR images, a finding that is similar to the enhancement pattern seen at contrast-enhanced CT. The area of the tumor with early enhancement and rapid washout indicates active growth, whereas the central area is composed mainly of loose connective tissue with an abundant intercellular matrix. Hyperattenuating areas in intrahepatic cholangiocarcinoma on delayed phase images may also be related to the fibrous stroma of the tumor (45,46), and cirrhotic cholangiocarcinoma with abundant fibrous stroma has been reported to correlate more closely with a somewhat poorer prognosis than does the noncirrhotic form (46,47). Not all cholangiocarcinomas manifest with the typical imaging pattern, and various atypical patterns are frequently seen. Homogeneous hypervascular enhancement is an uncommon finding but may be seen in a well-differentiated tumor with abundant tumor vasculature in the fibrotic stroma in the absence of remarkable necrosis. Prolonged enhancement may be attributed to the presence of the vascular fibrotic stroma (48). If a tumor manifests with central necrosis, which is common in metastatic adenocarcinoma but rare in cholangiocarcinoma (42), it may be very difficult to make a preoperative diagnosis. Mucinous carcinoma is one variant of cholangiocarcinoma that may show strong hyperintensity and centripetal enhancement on T2-weighted MR images, but it can and should be distinguished from a hemangioma at imaging on the basis of its continuous ragged rim enhancement, as opposed to the stronger and globular enhancement of the latter (49).

Several tumors or tumorlike conditions should be included in the differential diagnosis for a mass-forming cholangiocarcinoma. HCC with cirrhotic stroma, sclerosing HCC, and combined HCC-cholangiocarcinoma can all appear nearly identical to cholangiocarcinoma. Therefore, these three tumors should always be considered together, especially in patients with chronic liver disease (50–52). In addition, various tumors with abundant fibrous stroma, immature abscesses, metastasis from other sites, and hepatic tuberculosis may manifest with similar findings. In hepatic metastasis from an extrahepatic tumor, the area of central necrosis can be identified as a strongly hyperintense area on T2-weighted images and as a hypointense area on T1-weighted images, with delayed contrast material uptake on the hepatobiliary phase image. Such areas of central necrosis are not common in primary cholangiocarcinoma and can help differentiate metastatic lesions from a mass-forming cholangiocarcinoma. An organizing abscess is commonly seen in patients with intrahepatic stone disease and may be differentiated from cholangiocarcinoma on the basis of its thick enhancing wall with central cystic change, findings that are uncommon in cholangiocarcinoma. An immature abscess manifesting at a very early stage may mimic a cholangiocarcinoma, especially in a patient at high risk for cholangiocarcinoma. In these cases, findings on serial follow-up scans are useful in making the correct diagnosis. Hepatic tuberculosis can be distinguished from cholangiocarcinoma on the basis of its multilayered appearance (Fig 8).

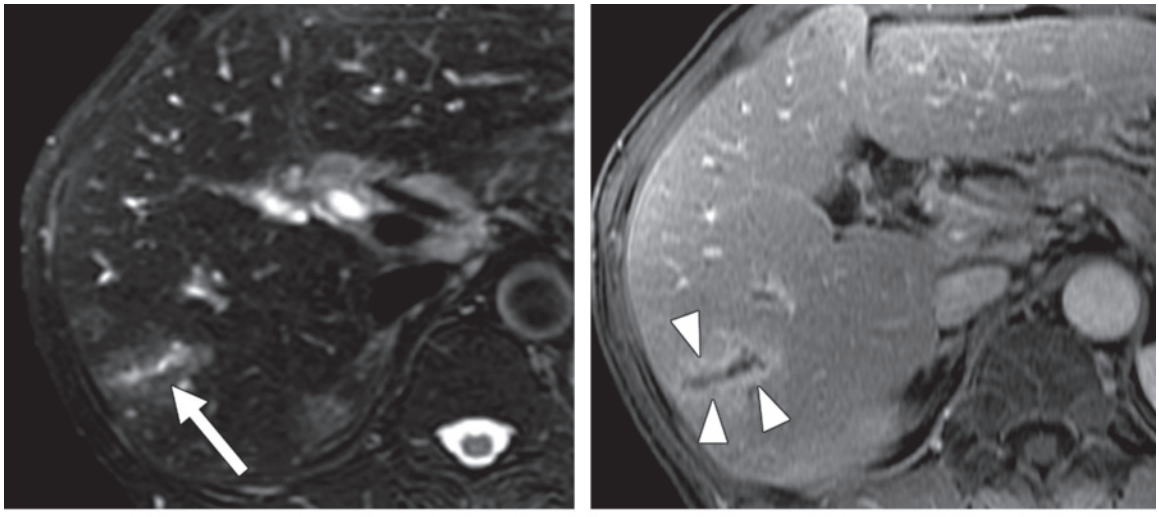

a. b.

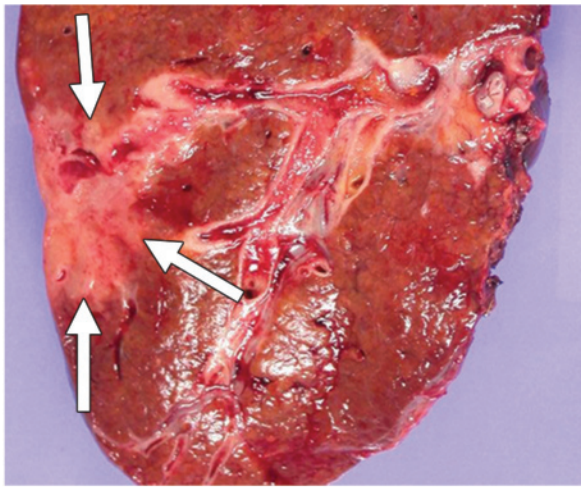

c.

Figure 9. Periductal infiltrating cholangiocarcinoma. **(a)** Axial T2-weighted MR image shows a dilated peripheral intrahepatic duct with a slightly hyperintense lesion around the duct (arrow). **(b)** Contrast-enhanced equilibrium phase MR image shows periductal enhancement around the dilated intrahepatic duct (arrowheads). **(c)** Photograph of the gross specimen reveals a periductal infiltrating tumor (arrows) along the irregularly dilated intrahepatic duct.

Periductal Infiltrating Type

Teaching Point

Periductal infiltrating cholangiocarcinoma is characterized by growth along a dilated or narrowed bile duct without mass formation and manifests as an elongated, spiculated, or branch-like abnormality. At US, infiltrating type cholangiocarcinoma appears as a small, masslike lesion or diffuse bile duct thickening with or without obliteration of the bile duct lumen depending on tumor extent (53,54). At CT and MR imaging, diffuse periductal thickening and increased enhancement due to tumor infiltration can be seen, with an abnormally dilated or irregularly narrowed duct and peripheral ductal dilatation (Fig 9). This type of tumor is rare in intrahepatic cholangiocarcinoma, but most hilar cholangiocarcinomas are of this type (Fig 10) (13,55,56). In the periphery of the liver, a combination of the periductal and mass-forming types is more common than a purely periductal infiltrating lesion.

The differential diagnosis for a periductal infiltrating cholangiocarcinoma includes periportal lymphangitic metastasis from the extrahepatic tumor (57). The latter finding can be distinguished from periductal cholangiocarcinoma on the basis of *(a)* the absence of ductal dilatation and *(b)* diffuse involvement of both sides of the liver. In contrast, periductal cholangiocarcinoma tends to be localized to one segment or lobe and manifests with ductal dilatation, a finding that is indicative of biliary disease. Peribiliary cysts may look similar to cholangiocarcinoma, but they can easily be differentiated from periductal infiltrating cholangiocarcinomas on the basis of the presence of multiple peribiliary cysts with discrete margins and the absence of ductal dilatation or soft-tissue lesions.

The early diagnosis of periductal infiltrating cholangiocarcinoma can be very difficult because

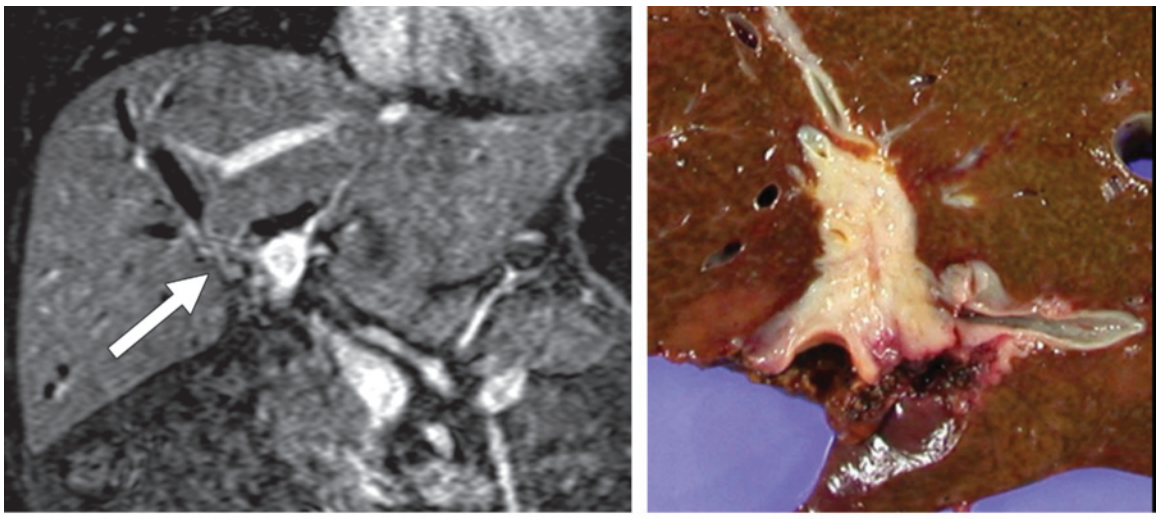

a. b.

Figure 10. Periductal infiltrating hilar cholangiocarcinoma. **(a)** Coronal T2-weighted MR image shows irregular ductal wall thickening along a narrowed hilar bile duct (arrow). **(b)** Photograph of the gross specimen reveals an elongated and branchlike tumor along the bile duct.

Table 2
Classification of BilIN

Classification	Description
BilIN-1	Low-grade dysplasia of biliary epithelium, mild cellular-nuclear atypia suggestive of neoplasia
BilIN-2	High-grade dysplasia of biliary epithelium, cellular-nuclear atypia evident but insufficient to represent overt malignancy
BilIN-3	Carcinoma in situ, cellular-nuclear atypia representing overt malignancy

Sources.—References 15 and 60.

this entity may begin as a benign-looking stricture. The correct diagnosis of peribiliary cholangiocarcinoma depends on differentiating the benign focal stricture from a true malignancy. Findings of *(a)* a long-segment stricture with an irregular margin, asymmetric narrowing, ductal enhancement, and lymph node enlargement and *(b)* a periductal soft-tissue lesion suggest a malignant stricture (58,59).

Intraductal Type

Intraductal cholangiocarcinoma is an intriguing type of cholangiocarcinoma because it has a variety of imaging features, grows slowly, and has a relatively favorable prognosis. Imaging patterns include *(a)* diffuse and marked ductectasia with a grossly visible papillary mass, *(b)* diffuse and marked ductectasia without a visible mass, *(c)* an intraductal polypoid mass within localized ductal dilatation, *(d)* intraductal castlike lesions within a mildly dilated duct, and *(e)* a focal stricture-like lesion with mild proximal ductal dilatation.

Teaching Point

Intraductal cholangiocarcinoma may be classified as either macroscopic or microscopic. Microscopic lesions may represent the early form of typical cholangiocarcinoma, whereas macroscopic lesions may represent a distinct pathologic entity. Macroscopic lesions manifest as either papillary or tubular polypoid lesions. Intraductal papillary neoplasm of the biliary tract is currently thought to be the counterpart of intraductal papillary mucinous neoplasm of the pancreas and is frequently associated with marked mucin production. Microscopic lesions are tumors with flat or micropapillary growth associated with BilIN, which is thought to be a precursor of cholangiocarcinoma in a multistep cholangiocarcinogenesis involving low-grade (BilIN-1) and high-grade (BilIN-2) intraepithelial dysplasia and carcinoma in situ (BilIN-3) (Table 2). BilIN is regarded as a counterpart of pancreatic intraepithelial neoplasia (15,60–64).

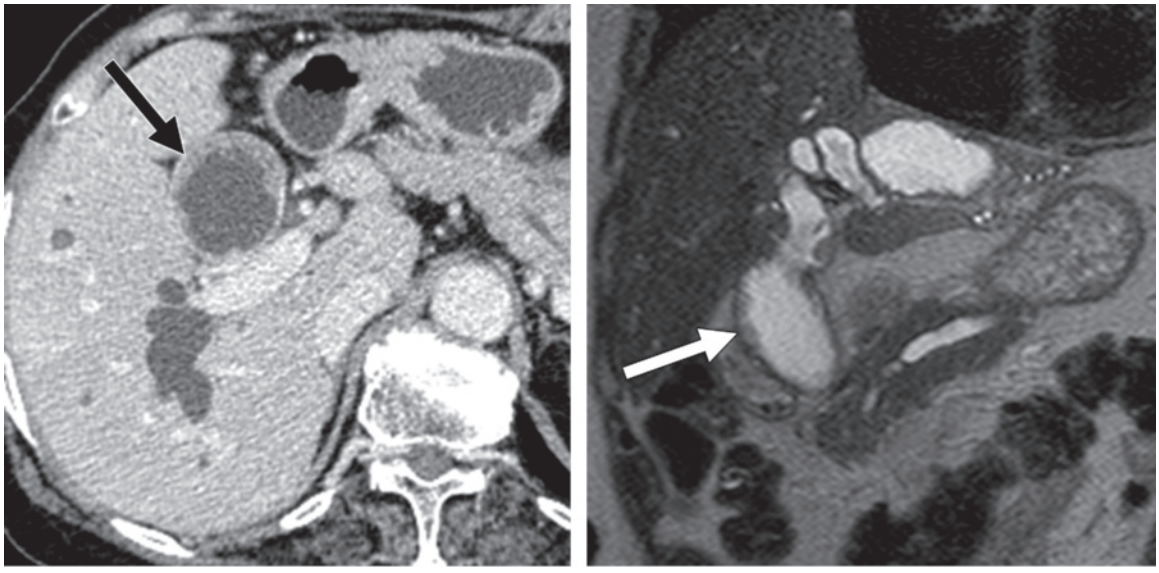

a. b.

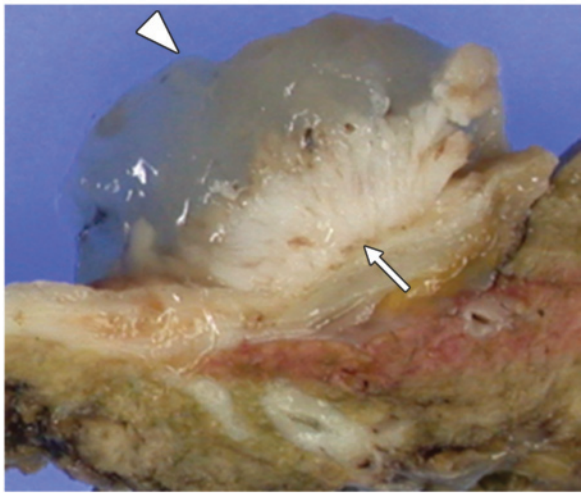

c.

Figure 11. Intraductal papillary neoplasm of the biliary tract with marked mucin production. **(a, b)** Contrast-enhanced CT scan **(a)** and T2-weighted MR image **(b)** show a markedly dilated intrahepatic duct with mural nodules or irregular wall thickening (arrow). **(c)** Photograph of the gross specimen reveals an intraluminal plaquelike or papillary mass (arrow) and mucin (arrowhead).

The most distinguishable imaging pattern of the first type of intraductal cholangiocarcinoma is diffuse ductal dilatation with multifocal superficial spreading papillary or plaquelike masses at CT or MR imaging (Fig 11) (65). These papillary tumors may look like seaweed or coral at cholangioscopy and gross examination. At US, an intraductal polypoid lesion is echogenic relative to the surrounding liver. At precontrast CT, an intraductal mass appears as a lesion within the dilated bile duct that is hypo- or isoattenuating relative to the surrounding liver. After contrast medium administration, the intraductal tumor shows enhancement. This lesion is usually confined to the bile duct wall, so that the wall will appear intact at US and CT (40,66,67). In some cases, only marked intrahepatic bile duct dilatation with no obstructive mass or stricture can be detected at imaging. These imaging findings can be explained on the basis of copious mucin production. Because mucin is usually anechoic at US and appears isoattenuating relative to water at precontrast CT, it is hard to detect at US or CT (66). Papillary growth of the tumor is clearly visible on a gross specimen (Fig 11c). Tumors can easily slough from the surface and may produce sludge or stones. In the second pattern of intraductal cholangiocarcinoma, a diffuse and marked ductectasia is present as in the first pattern, but a grossly visible mass is not present at CT, MR imaging, or even gross examination. This is either because of the micropapillary nature of the tumor (Fig 12) or because of the limited spatial resolution of the imaging modalities. The third pattern of intraductal tumors manifests as localized ductal dilatation with an intraductal mass. An intraductal papillary mass is also usually present, but mucin secretion is not remarkable, so that the distal ductal dilatation is not prominent (Fig 13). This type of tumor can be distinguished from an HCC invading the bile duct on the basis of identification of the mass outside the ductal system, hypervascularity at dynamic imaging, the pres-

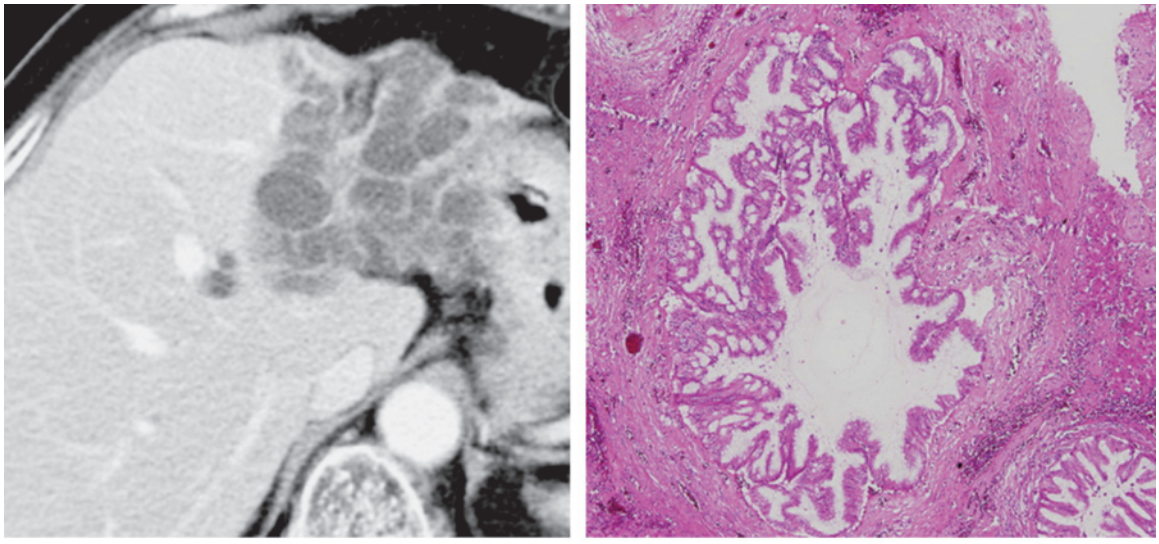

a. b.

Figure 12. BilIN-3. **(a)** Axial contrast-enhanced CT scan shows diffuse ductal dilatation in the left hepatic lobe through the common bile duct, with no visible intraductal mass. **(b)** Photomicrograph (original magnification, ×40; H-E stain) shows micropapillary tumors throughout the bile ducts. These findings are compatible with the micropapillary form of BilIN-3 (carcinoma in situ).

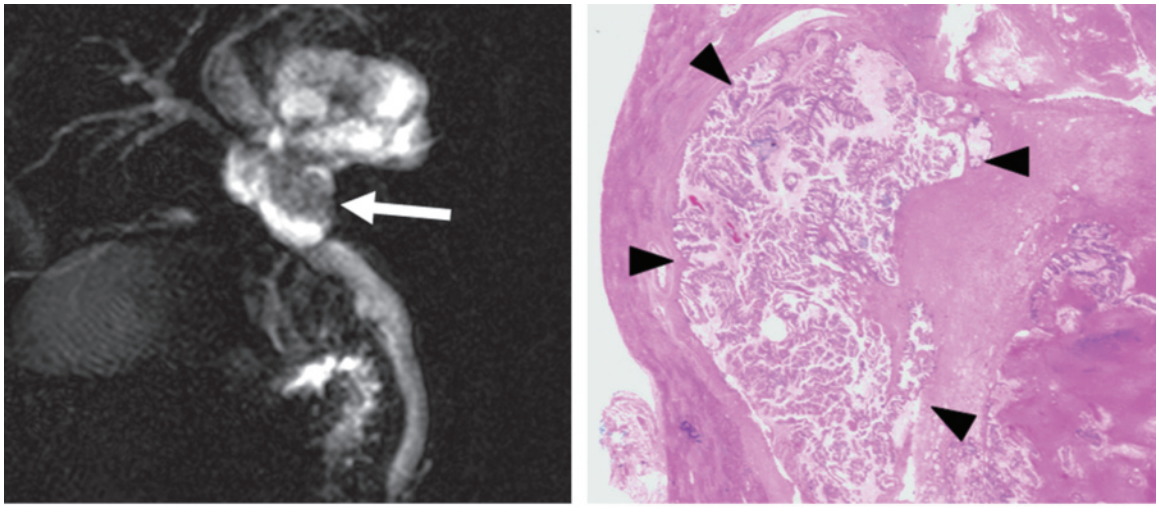

a. b.

Figure 13. Intraductal papillary cholangiocarcinoma. **(a)** MR cholangiopancreatogram shows an intraductal polypoid mass with localized ductal dilatation (arrow). **(b)** Photomicrograph (original magnification, ×1; H-E stain) shows an intraductal growth type mass with focal ductal dilatation (arrowheads).

ence of a prominent fibrous capsule or pseudocapsule, and other imaging features favoring HCC (22). This type of intraductal tumor may also be confused with an intraductal masslike stone. The absence of contrast enhancement and the high attenuation at precontrast CT are useful in making the diagnosis of an intraductal masslike stone, whereas an enhancing polypoid mass with asymmetric adjacent bile duct wall thickening is suggestive of an intraductal tumor (68). However, the presence of hepatolithiasis does not exclude the coexistence of an intraductal tumor, and one must be careful not to miss a coexistent intraductal tumor in cases of hepatolithiasis (13). A biliary cystadenoma or cystadenocarcinoma may manifest as a cyst that contains intracystic lesions and may mimic an intraductal tumor (69), but the absence of ductal communication helps in making the correct diagnosis. The fourth pattern is one of the most

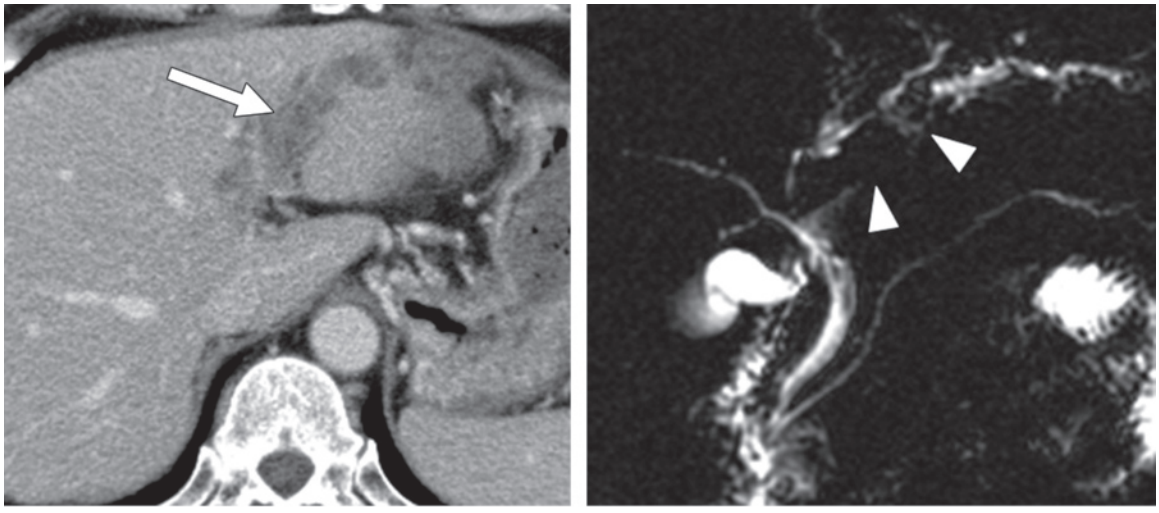

a. b.

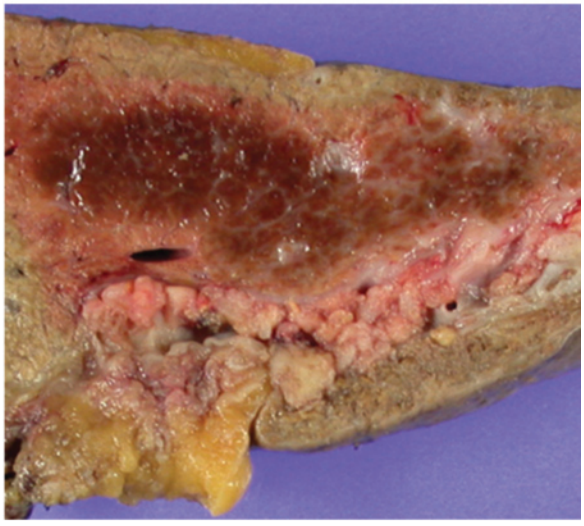

c.

Figure 14. Intraductal cholangiocarcinoma. **(a)** CT scan shows a soft-tissue component filling a mildly dilated duct (arrow). **(b)** MR cholangiopancreatogram shows the mildly dilated duct with irregularities that mimic impacted stones (arrowheads). **(c)** Photograph of the gross specimen reveals a dilated bile duct with innumerable impacted small polypoid lesions representing tubular carcinomas without mucin production.

difficult forms to diagnose correctly at imaging. It manifests as an area of mild ductal dilatation filled with intraductal soft-tissue material, which may show mild enhancement at CT or MR imaging (Fig 14). Impacted stones in the intrahepatic bile duct may appear similar to this type of tumor, but the presence of calcifications and the absence of contrast enhancement may be helpful in making the correct diagnosis (intraductal impacted stones). However, as mentioned before, the identification of hepatolithiasis does not exclude a coexistent carcinoma. The last pattern of intraductal cholangiocarcinoma manifests as a focal stricture-like lesion with mild proximal ductal dilatation and no demonstrable mass (Fig 15). The stricture may be a secondary finding of the underlying inflammation and fibrotic stricture or may itself represent a small tumor. The differential diagnosis for this type of lesion includes a benign stricture and intraepithelial dysplasia (BilIN-1 or BilIN-2). In patients with intrahepatic stone disease, most focal strictures turn out to be benign; nevertheless, these strictures should be viewed with a high degree of suspicion for malignancy.

Conclusions

Current evidence suggests that the prevalence of cholangiocarcinoma is increasing worldwide despite some controversy over anatomic classification. Liver flukes and hepatolithiasis are common risk factors in eastern Asia, whereas PSC, liver cirrhosis, alcohol-related liver disease, and diabetes are relatively common risk factors in Western countries. Cholangiocarcinoma can be classified on the basis of gross morphologic features into mass-forming, periductal infiltrating, and intraductal types, and the imaging features may depend on the underlying causative risk factors (Table 3). Intraductal type cholangiocarcinoma can be subdivided on the basis of imaging findings, which include diffuse and marked ductectasia with a grossly visible papillary mass, diffuse and

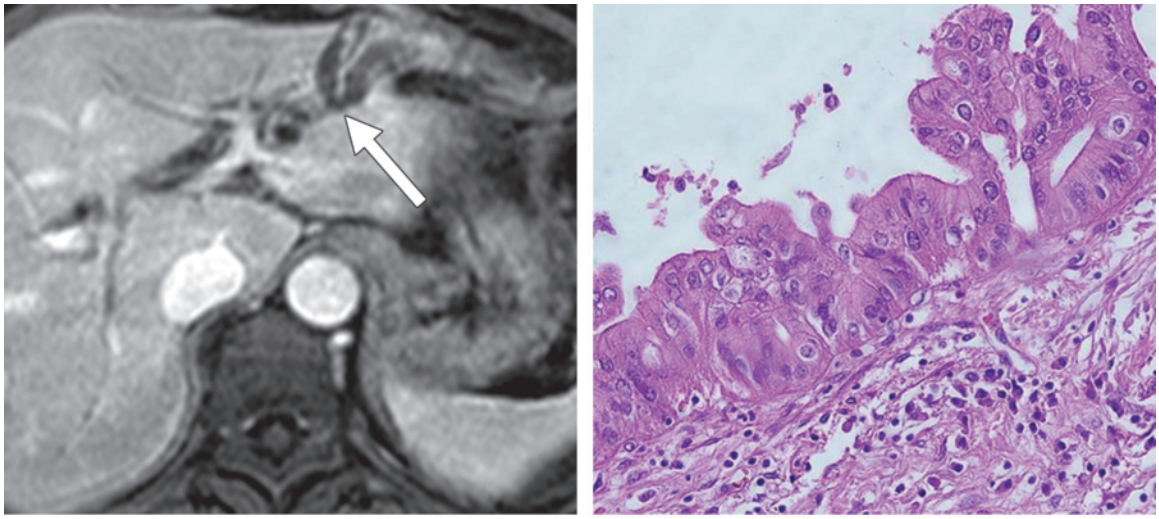

a. b.

Figure 15. BilIN with a focal ductal stricture. **(a)** Axial contrast-enhanced MR image show a focal stricture (arrow) with mild ductal dilatation. **(b)** Photomicrograph (original magnification, ×200; H-E stain) shows an intraepithelial carcinoma, also known as carcinoma in situ or BilIN-3, without subepithelial extension.

Table 3
Imaging Findings of Cholangiocarcinoma according to Morphologic Type

Morphologic Type	Imaging Findings		
	US	CT	MR Imaging
Mass-forming	Hyperehoic (larger than 3 cm), hypo- or isoechoic (less than 3 cm), peripheral hypoechoic rim (~35% of all tumors)	Homogeneous attenuation, irregular peripheral enhancement, gradual centripetal enhancement	Hyperintense at T2-weighted imaging, hypointense at T1-weighted imaging, peripheral and centripetal enhancement at dynamic contrast-enhanced imaging; associated findings: capsular retraction, satellite nodules, vascular encasement without gross tumor thrombus formation, hepatolithiasis
Periductal infiltrating	Small, masslike lesion or diffuse bile duct thickening with or without obliteration of the bile duct lumen	Diffuse periductal thickening with increased enhancement, abnormally dilated or irregularly narrowed duct	Diffuse periductal thickening with increased enhancement, abnormally dilated or irregularly narrowed duct
Intraductal	Localized or diffuse ductectasia with or without an echogenic intraductal polypoid lesion	Diffuse and marked ductal dilatation with an intraductal mass that is hypo- or isoattenuating relative to the surrounding liver at precontrast CT and enhances at contrast-enhanced CT, marked intrahepatic duct dilatation with no mass or stricture, an intraductal polypoid mass within localized ductal dilatation, an intraductal castlike lesion within a mildly dilated duct, or a focal stricture-like lesion with mild proximal ductal dilatation	Diffuse and marked ductal dilatation with an intraductal mass that enhances at contrast-enhanced MR imaging, marked intrahepatic duct dilatation with no mass or stricture, an intraductal polypoid mass within localized ductal dilatation, an intraductal castlike lesion within a mildly dilated duct, or a focal stricture-like lesion with mild proximal ductal dilatation

marked ductectasia with no visible mass, an intraductal polypoid mass within localized ductal dilatation, intraductal castlike lesions within a mildly dilated duct, and a focal stricture-like lesion with mild proximal ductal dilatation. With pathologic correlation, these imaging findings can be related to emerging pathologic concepts of intraductal papillary neoplasm of the biliary tract and BilIN. Morphologic classification is useful for interpreting imaging findings and understanding tumor behavior. Finally, it is important to consider the various tumorous and nontumorous diseases when developing the differential diagnosis.

References

1. Patel T, Singh P. Cholangiocarcinoma: emerging approaches to a challenging cancer. Curr Opin Gastroenterol 2007;23(3):317–323.
2. Khan SA, Thomas HC, Davidson BR, Taylor-Robinson SD. Cholangiocarcinoma. Lancet 2005;366 (9493):1303–1314.
3. Lazaridis KN, Gores GJ. Cholangiocarcinoma. Gastroenterology 2005;128(6):1655–1667.
4. Shaib Y, El-Serag HB. The epidemiology of cholangiocarcinoma. Semin Liver Dis 2004;24(2): 115–125.
5. Liver Cancer Study Group of Japan. Classification of primary liver cancer. Tokyo, Japan: Kanehara, 1997.
6. Patel T. Cholangiocarcinoma. Nat Clin Pract Gastroenterol Hepatol 2006;3(1):33–42.
7. Welzel TM, McGlynn KA, Hsing AW, O'Brien TR, Pfeiffer RM. Impact of classification of hilar cholangiocarcinomas (Klatskin tumors) on the incidence of intra- and extrahepatic cholangiocarcinoma in the United States. J Natl Cancer Inst 2006;98(12): 873–875.
8. Thamavit W, Bhamarapravati N, Sahaphong S, Vajrasthira S, Angsubhakorn S. Effects of dimethylnitrosamine on induction of cholangiocarcinoma in Opisthorchis viverrini-infected Syrian golden hamsters. Cancer Res 1978;38(12):4634–4639.
9. Choi D, Lim JH, Hong ST. Relation of cholangiocarcinomas to clonorchiasis and bile duct stones. Abdom Imaging 2004;29(5):590–597.
10. Zhou YM, Yin ZF, Yang JM, et al. Risk factors for intrahepatic cholangiocarcinoma: a case-control study in China. World J Gastroenterol 2008;14(4): 632–635.
11. Lee TY, Lee SS, Jung SW, et al. Hepatitis B virus infection and intrahepatic cholangiocarcinoma in Korea: a case-control study. Am J Gastroenterol 2008; 103(7):1716–1720.
12. Ahrendt SA, Nakeeb A, Pitt HA. Cholangiocarcinoma. Clin Liver Dis 2001;5(1):191–218.
13. Park HS, Lee JM, Kim SH, et al. CT differentiation of cholangiocarcinoma from periductal fibrosis in patients with hepatolithiasis. AJR Am J Roentgenol 2006;187(2):445–453.
14. Kim JH, Kim TK, Eun HW, et al. CT findings of cholangiocarcinoma associated with recurrent pyogenic cholangitis. AJR Am J Roentgenol 2006;187 (6):1571–1577.
15. Zen Y, Adsay NV, Bardadin K, et al. Biliary intraepithelial neoplasia: an international interobserver agreement study and proposal for diagnostic criteria. Mod Pathol 2007;20(6):701–709.
16. Campbell WL, Ferris JV, Holbert BL, Thaete FL, Baron RL. Biliary tract carcinoma complicating primary sclerosing cholangitis: evaluation with CT, cholangiography, US, and MR imaging. Radiology 1998;207(1):41–50.
17. Shaib YH, El-Serag HB, Nooka AK, et al. Risk factors for intrahepatic and extrahepatic cholangiocarcinoma: a hospital-based case-control study. Am J Gastroenterol 2007;102(5):1016–1021.
18. Welzel TM, Mellemkjaer L, Gloria G, et al. Risk factors for intrahepatic cholangiocarcinoma in a low-risk population: a nationwide case-control study. Int J Cancer 2007;120(3):638–641.
19. Kim SJ, Lee JM, Han JK, Kim KH, Lee JY, Choi BI. Peripheral mass-forming cholangiocarcinoma in cirrhotic liver. AJR Am J Roentgenol 2007;189(6): 1428–1434.
20. Zheng LX, Jia HB, Wu DQ, et al. Experience of congenital choledochal cyst in adults: treatment, surgical procedures and clinical outcome in the Second Affiliated Hospital of Harbin Medical University. J Korean Med Sci 2004;19(6):842–847.
21. Watanabe Y, Toki A, Todani T. Bile duct cancer developed after cyst excision for choledochal cyst. J Hepatobiliary Pancreat Surg 1999;6(3):207–212.
22. Jung AY, Lee JM, Choi SH, et al. CT features of an intraductal polypoid mass: differentiation between hepatocellular carcinoma with bile duct tumor invasion and intraductal papillary cholangiocarcinoma. J Comput Assist Tomogr 2006;30(2):173–181.
23. Neitlich JD, Topazian M, Smith RC, Gupta A, Burrell MI, Rosenfield AT. Detection of choledocholithiasis: comparison of unenhanced helical CT and endoscopic retrograde cholangiopancreatography. Radiology 1997;203(3):753–757.
24. Uchida M, Ishibashi M, Tomita N, Shinagawa M, Hayabuchi N, Okuda K. Hilar and suprapancreatic cholangiocarcinoma: value of 3D angiography and multiphase fusion images using MDCT. AJR Am J Roentgenol 2005;184(5):1572–1577.
25. Choi YH, Lee JM, Lee JY, et al. Biliary malignancy: value of arterial, pancreatic, and hepatic phase imaging with multidetector-row computed tomography. J Comput Assist Tomogr 2008;32(3):362–368.

26. Tillich M, Mischinger HJ, Preisegger KH, Rabl H, Szolar DH. Multiphasic helical CT in diagnosis and staging of hilar cholangiocarcinoma. AJR Am J Roentgenol 1998;171(3):651–658.
27. Kim TK, Choi BI, Han JK, Jang HJ, Cho SG, Han MC. Peripheral cholangiocarcinoma of the liver: two-phase spiral CT findings. Radiology 1997;204(2):539–543.
28. Kamel IR, Liapi E, Fishman EK. Liver and biliary system: evaluation by multidetector CT. Radiol Clin North Am 2005;43(6):977–997, vii.
29. Lacomis JM, Baron RL, Oliver JH 3rd, Nalesnik MA, Federle MP. Cholangiocarcinoma: delayed CT contrast enhancement patterns. Radiology 1997;203(1):98–104.
30. Maetani Y, Itoh K, Watanabe C, et al. MR imaging of intrahepatic cholangiocarcinoma with pathologic correlation. AJR Am J Roentgenol 2001;176(6):1499–1507.
31. Kim JY, Lee JM, Han JK, et al. Contrast-enhanced MRI combined with MR cholangiopancreatography for the evaluation of patients with biliary strictures: differentiation of malignant from benign bile duct strictures. J Magn Reson Imaging 2007;26(2):304–312.
32. Guarise A, Venturini S, Faccioli N, Pinali L, Morana G. Role of magnetic resonance in characterising extrahepatic cholangiocarcinomas. Radiol Med 2006;111(4):526–538.
33. Manfredi R, Barbaro B, Masselli G, Vecchioli A, Marano P. Magnetic resonance imaging of cholangiocarcinoma. Semin Liver Dis 2004;24(2):155–164.
34. Park HS, Lee JM, Choi JY, et al. Preoperative evaluation of bile duct cancer: MRI combined with MR cholangiopancreatography versus MDCT with direct cholangiography. AJR Am J Roentgenol 2008;190(2):396–405.
35. Sasaki A, Aramaki M, Kawano K, et al. Intrahepatic peripheral cholangiocarcinoma: mode of spread and choice of surgical treatment. Br J Surg 1998;85(9):1206–1209.
36. Yamamoto M, Takasaki K, Yoshikawa T, Ueno K, Nakano M. Does gross appearance indicate prognosis in intrahepatic cholangiocarcinoma? J Surg Oncol 1998;69(3):162–167.
37. Isaji S, Kawarada Y, Taoka H, Tabata M, Suzuki H, Yokoi H. Clinicopathological features and outcome of hepatic resection for intrahepatic cholangiocarcinoma in Japan. J Hepatobiliary Pancreat Surg 1999;6(2):108–116.
38. Wernecke K, Henke L, Vassallo P, et al. Pathologic explanation for hypoechoic halo seen on sonograms of malignant liver tumors: an in vitro correlative study. AJR Am J Roentgenol 1992;159(5):1011–1016.
39. Wibulpolprasert B, Dhiensiri T. Peripheral cholangiocarcinoma: sonographic evaluation. J Clin Ultrasound 1992;20(5):303–314.
40. Lim JH. Cholangiocarcinoma: morphologic classification according to growth pattern and imaging findings. AJR Am J Roentgenol 2003;181(3):819–827.
41. Han JK, Choi BI, Kim AY, et al. Cholangiocarcinoma: pictorial essay of CT and cholangiographic findings. RadioGraphics 2002;22(1):173–187.
42. Ros PR, Buck JL, Goodman ZD, Ros AM, Olmsted WW. Intrahepatic cholangiocarcinoma: radiologic-pathologic correlation. Radiology 1988;167(3):689–693.
43. Choi BI, Lee JH, Han MC, Kim SH, Yi JG, Kim CW. Hilar cholangiocarcinoma: comparative study with sonography and CT. Radiology 1989;172(3):689–692.
44. Vilgrain V, Van Beers BE, Flejou JF, et al. Intrahepatic cholangiocarcinoma: MRI and pathologic correlation in 14 patients. J Comput Assist Tomogr 1997;21(1):59–65.
45. Valls C, Guma A, Puig I, et al. Intrahepatic peripheral cholangiocarcinoma: CT evaluation. Abdom Imaging 2000;25(5):490–496.
46. Asayama Y, Yoshimitsu K, Irie H, et al. Delayed-phase dynamic CT enhancement as a prognostic factor for mass-forming intrahepatic cholangiocarcinoma. Radiology 2006;238(1):150–155.
47. Kajiyama K, Maeda T, Takenaka K, Sugimachi K, Tsuneyoshi M. The significance of stromal desmoplasia in intrahepatic cholangiocarcinoma: a special reference of "scirrhous-type" and "nonscirrhous-type" growth. Am J Surg Pathol 1999;23(8):892–902.
48. Yoshida Y, Imai Y, Murakami T, et al. Intrahepatic cholangiocarcinoma with marked hypervascularity. Abdom Imaging 1999;24(1):66–68.
49. Hayashi M, Matsui O, Ueda K, et al. Imaging findings of mucinous type of cholangiocellular carcinoma. J Comput Assist Tomogr 1996;20(3):386–389.
50. Lee WJ, Lim HK, Jang KM, et al. Radiologic spectrum of cholangiocarcinoma: emphasis on unusual manifestations and differential diagnoses. RadioGraphics 2001;21(spec no):S97–S116.
51. Zuo HQ, Yan LN, Zeng Y, et al. Clinicopathological characteristics of 15 patients with combined hepatocellular carcinoma and cholangiocarcinoma. Hepatobiliary Pancreat Dis Int 2007;6(2):161–165.
52. Nishie A, Yoshimitsu K, Asayama Y, et al. Detection of combined hepatocellular and cholangiocarcinomas on enhanced CT: comparison with histologic findings. AJR Am J Roentgenol 2005;184(4):1157–1162.
53. Mittelstaedt CA. Ultrasound of the bile ducts. Semin Roentgenol 1997;32(3):161–171.
54. Robledo R, Muro A, Prieto ML. Extrahepatic bile duct carcinoma: US characteristics and accuracy in demonstration of tumors. Radiology 1996;198(3):869–873.
55. Lim JH, Park CK. Pathology of cholangiocarcinoma. Abdom Imaging 2004;29(5):540–547.

56. Han JK, Lee JM. Intrahepatic intraductal cholangiocarcinoma. Abdom Imaging 2004;29(5):558–564.
57. Tada H, Morimoto M, Shima T, et al. Progressive jaundice due to lymphangiosis carcinomatosa of the liver: CT appearance. J Comput Assist Tomogr 1996;20(4):650–652.
58. Park MS, Kim TK, Kim KW, et al. Differentiation of extrahepatic bile duct cholangiocarcinoma from benign stricture: findings at MRCP versus ERCP. Radiology 2004;233(1):234–240.
59. Patel T. Increasing incidence and mortality of primary intrahepatic cholangiocarcinoma in the United States. Hepatology 2001;33(6):1353–1357.
60. Zen Y, Aishima S, Ajioka Y, et al. Proposal of histological criteria for intraepithelial atypical/proliferative biliary epithelial lesions of the bile duct in hepatolithiasis with respect to cholangiocarcinoma: preliminary report based on interobserver agreement. Pathol Int 2005;55(4):180–188.
61. Zen Y, Fujii T, Itatsu K, et al. Biliary papillary tumors share pathological features with intraductal papillary mucinous neoplasm of the pancreas. Hepatology 2006;44(5):1333–1343.
62. Kloppel G, Kosmahl M. Is the intraductal papillary mucinous neoplasia of the biliary tract a counterpart of pancreatic papillary mucinous neoplasm? J Hepatol 2006;44(2):249–250.
63. Zen Y, Sasaki M, Fujii T, et al. Different expression patterns of mucin core proteins and cytokeratins during intrahepatic cholangiocarcinogenesis from biliary intraepithelial neoplasia and intraductal papillary neoplasm of the bile duct: an immunohistochemical study of 110 cases of hepatolithiasis. J Hepatol 2006;44(2):350–358.
64. Lim JH, Yoon KH, Kim SH, et al. Intraductal papillary mucinous tumor of the bile ducts. RadioGraphics 2004;24(1):53–67.
65. Kawakatsu M, Vilgrain V, Zins M, Vullierme M, Belghiti J, Menu Y. Radiologic features of papillary adenoma and papillomatosis of the biliary tract. Abdom Imaging 1997;22(1):87–90.
66. Lim JH, Yi CA, Lim HK, Lee WJ, Lee SJ, Kim SH. Radiological spectrum of intraductal papillary tumors of the bile ducts. Korean J Radiol 2002;3(1):57–63.
67. Lee JW, Han JK, Kim TK, et al. CT features of intraductal intrahepatic cholangiocarcinoma. AJR Am J Roentgenol 2000;175(3):721–725.
68. Lim JH, Kim MH, Kim TK, et al. Papillary neoplasms of the bile duct that mimic biliary stone disease. RadioGraphics 2003;23(2):447–455.
69. Shimada M, Takenaka K, Gion T, et al. Treatment strategy for patients with cystic lesions mimicking a liver tumor: a recent 10-year surgical experience in Japan. Arch Surg 1998;133(6):643–646.

This article meets the criteria for 1.0 credit hour in category 1 of the AMA Physician's Recognition Award. To obtain credit, see accompanying test at http://www.rsna.org/education/rg_cme.html.

RadioGraphics

Varying Appearances of Cholangiocarcinoma: Radiologic-Pathologic Correlation

Yong Eun Chung, MD, et al

RadioGraphics 2009; 29:683–700 • **Published online** 10.1148/rg.293085729 • **Content Codes:** GI OI

Page 684
A recent epidemiologic study addressed this misclassification issue but showed that the prevalence of intrahepatic cholangiocarcinoma has actually increased, even after the exclusion of the misclassified cases (7).

Page 684
There are a number of recognized risk factors for cholangiocarcinoma that all share the common feature of chronic biliary inflammation (Table 1).

Page 688
The typical CT features of a mass-forming cholangiocarcinoma include homogeneous attenuation, irregular peripheral enhancement with gradual centripetal enhancement, capsular retraction, the presence of satellite nodules, and vascular encasement without the formation of a grossly visible tumor thrombus (Fig 6a–6c) (40–43).

Page 692
Periductal infiltrating cholangiocarcinoma is characterized by growth along a dilated or narrowed bile duct without mass formation and manifests as an elongated, spiculated, or branchlike abnormality.

Page 693
Imaging patterns include (a) diffuse and marked ductectasia with a grossly visible papillary mass, (b) diffuse and marked ductectasia without a visible mass, (c) an intraductal polypoid mass within localized ductal dilatation, (d) intraductal castlike lesions within a mildly dilated duct, and (e) a focal stricture-like lesion with mild proximal ductal dilatation.